EARTH OBSERVATION AND GEOMATICS ENGINEERING
website: https://eoge.ut.ac.ir

Optimizing the regularization parameters of prior information in sparse coding-based multispectral image fusion

Afshin Asefpour Vakilian*, Mohammad Reza Saradjian

School of Surveying and Geospatial Engineering, University College of Engineering, University of Tehran, Tehran, Iran

Article history:
Received: 25 March 2020, Received in revised form: 26 August 2020, Accepted: 29 August 2020

ABSTRACT

Advanced sparse coding-based image fusion methods use some prior information to fuse low-resolution multispectral (LR-MS) and panchromatic images to create a high-resolution multispectral image (HR-MS). This information mainly includes a sparsity term, spectral unmixing, and nonlocal similarities. These prior terms are usually considered in the sparse optimization problem as constraints with specific regularization parameters. During the optimization, the regularization parameter of each prior term is optimized by considering the other two prior terms as constants. This study aims to simultaneously optimize the regularization parameters of prior terms in a sparse coding image fusion method to construct an HR-MS from input LR-MS and Pan images. Several optimization methods, including particle swarm optimization, ant colony optimization, differential evolution, and genetic algorithm were used to optimize the regularization parameters. The results showed that particle swarm optimization had the highest performance in increasing the peak signal-to-noise ratio on the dataset available from the study area. The advantages of the proposed optimized sparse coding (OSC) approach are the ability to, 1) preserve spatial details while eliminating spectral distortions, 2) simultaneously optimize the regularization parameters of prior terms in a sparse coding image fusion framework, 3) considering nonlocal similarities to enhance fusion result, and 4) promising fusion results over heterogeneous regions with highly spectral variations. The relative dimensionless global error in synthesis, spectral angle mapper, universal image quality index, and peak signal to noise ratio criteria were at least 0.76, 1.16, 0.0257, and 2.68 better than those achieved by conventional PS methods, i.e., Gram-Schmidt, Brovey transform, generalized intensity-hue-saturation, smoothing filter-based intensity modulation, and a novel sparse coding-based image fusion method. According to the results, better preservation of spatial details and lower spectral distortions can be achieved using the proposed OSC approach.

KEYWORDS

High-resolution multispectral image

Particle swarm optimization

Spectral unmixing

Nonlocal similarity

Optimized sparse coding

1. Introduction

Remote sensing image fusion involves integrating the geometric detail of a high-resolution image, e.g., panchromatic (Pan), and spectral information of a low-resolution image, e.g., multispectral (MS), to produce a high-resolution MS image (Zhang, 2004). Image fusion can be performed at three levels: pixel level, feature level, and decision level. Among them, decision-level fusion is a high-level information fusion (Gunatilaka and Baertlein, 2001), which is less explored and is a hot spot in information fusion (Xiao et al., 2020a).

Pixel-level image fusion directly combines the original information in the source images, aiming to synthesize a fused image that is more informative for visual perception and computer processing. Many applications that require analysis of two or more images of a scene have been benefited from pixel-level image fusion (Li et al., 2017; Kulkarni and Rege, 2020). Depending on the application, pixel-level image fusion methods fall into spatial, spectral, model-based, and hybrid categories (Kaur et al., 2021). Spatial fusion methods preserve spatial content and are used

* Corresponding author
E-mail addresses: Afshin.asefpour@ut.ac.ir (A. Asefpour Vakilian); sarajian@ut.ac.ir (M. R. Saradjian)
DOI: 10.22059/eoge.2021.323695.1094

when geometric information is required; However, spectral fusion methods are suitable for spectral unmixing when separation of object classes is essential (Witharana et al., 2020). Hybrid fusion methods benefit from both spatial and spectral fusion methods and attempt to keep spectral characteristics while adding up geometric information to the fusion result (Yilmaz et al., 2020). Model-based fusion methods use statistical or numerical models to develop fused images (Dadrass Javan et al., 2021).

Feature-level image fusion is an intermediate-level fusion process based on the feature information extracted from the original information of each source for comprehensive analysis and processing (Rajah et al., 2018). The main idea of this type of fusion is first to extract useful features from the original multi-modal image and then merge these features into new feature vectors for further processing (Xiao et al., 2020b).

Regarding decision-level image fusion in remote sensing, researchers combine various types of current information and prior knowledge to provide suitable decisions on the gray levels of the resulting image (Li et al., 2018). In general, decision-level fusion is more reliable than the other two and can better overcome the shortcomings of each sensor. For other fusion levels, the failure of one sensor means the failure of the entire system. Compared with pixel-level fusion (Li et al., 2017) and feature-level fusion (Nirmala and Vaidehi, 2015), the decision-level fusion has the best real-time performance. However, the main drawback of this method is information loss. Before the fusion process, each sensor completes the goal of the decision-making. Then, according to some specific fusion criteria and the credibility of each decision-making process, it will make the best decision. Interested readers are encouraged to study the work of Dadrass Javan et al. (2021) for further background information in the field of image fusion methods.

Many studies have been reported on the limitations of existing fusion techniques (Zhang, 2004). The most significant problem is spectral distortion (Metwalli et al., 2009; Eghbalian and Ghassemian, 2018). Moreover, the fusion performance often depends on the operator's fusion experience and the dataset being fused. No automatic solution has been reported to produce high-quality fusion results for all available datasets. A wide variety of techniques have been developed for reducing spectral distortion and improving the fusion quality, each specific to a particular fusion approach or image dataset. By selecting a proper fusion technique and applying an appropriate adjustment strategy, successful results can be achieved. Nonetheless, when traditional fusion and adjustment techniques are used for the newer imaging sensors, remarkable spectral distortion becomes critical. For the new satellite images, a major reason for spectral distortion is the wavelength extension of the Pan image.

Bayesian frameworks have been introduced to minimize the drawbacks in spatial-spectral image fusion processes (Wei et al., 2015). These methods integrate posterior distribution based on prior knowledge to achieve accurate estimation. As a pioneering work, Hardie et al. (2004) used the maximum a posteriori (MAP)-based framework to fuse a low spatial resolution hyperspectral image (LR-HS) and a high spatial resolution multispectral image (HR-MS). Akhtar et al. (2015) used Bayesian sparse representation to solve the fusion problem. They provided the probability distributions of spectral basis with the Beta process and then utilized the resulting distributions to calculate sparse coefficients of the HR-HS. Xu et al. (2019) extracted the nonlocal similar patches to form a nonlocal patch tensor (NPT) for creating an HR-HS. They proposed a novel tensor-tensor product (t-product)-based tensor sparse representation to model the extracted NPTs. Then, they constructed the relationship between the HR-HS and LR-HS using the t-product, which allowed to design a unified objective function to incorporate the nonlocal similarity, tensor dictionary learning, and tensor sparse coding.

The matrix factorization has also been widely used to fuse LR-HS and HR-MS (Song et al., 2014). Since the HR-HS only contains limited pure spectral signatures (Iordache et al., 2011), the HR-HS can be approximately obtained by the spectral basis multiplied by the coefficients. Kawakami et al. (2011) used a sparse representation before learning the spectral basis from the LR-HS and performed sparse coding on the HR-MS to estimate the coefficients. Some studies have utilized the spatial structures of the HR-HS to regularize the fusion problem for better using the prior information of the HR-HS. As an example, Akhtar et al. (2014) obtained the coefficients with the simultaneous greedy pursuit algorithm for each local patch, utilizing the similarities of spectral pixels in the local patch in the HR-HS. Dong et al. (2016) used a nonnegative dictionary-learning algorithm to learn the spectral basis and estimated the coefficients using the structured sparse coding approach. They utilized the nonlocal similarities of the HR-HS and reported good fusion results. Dian et al. (2019) utilized sparsity, spectral (spectral unmixing), and spatial (nonlocal similarities) prior terms from the HR-HS in an optimization problem simultaneously. They proposed a spatial-spectral sparse representation technique to fuse an HR-MS and LR-HS with the same scenario. They formulated the fusion problem as the estimation of spectral basis and coefficients from the LR-HS and HR-MS. During the optimization process, the regularization parameter of each prior term was optimized by considering the other two prior terms as constants.

Different methods were used in this paper to optimize the regularization parameters of prior terms to select the best

candidate in the optimization step. Particle swarm optimization (PSO), ant colony optimization (ACO), differential evolution (DE), and genetic algorithm (GA) are among the well-known optimization methods that are used in the optimization step of this paper. PSO is one of the well-known nature-inspired optimization methods starting with creating a random population where each component in nature is a different set of decision variables whose optimal values should be provided in an iterative way. Each component represents a vector in the problem-solving space. The algorithm includes a velocity vector in addition to the position vector, which forces the population to change their positions in the search space. The velocity consists of two vectors called p and p_g. p is the best position that a particle has ever reached, and p_g is the best position that another particle in its neighborhood has ever reached. In this algorithm, each particle provides a solution in each iteration. The best result in the population during the iterations is considered as the optimized value (Yang, 2020).

Ant colony optimization (ACO) considers a simulation of ants producing pheromone when they find food on their way back. Other ants follow the pheromone produced by the ants, eventually choosing a path with stronger pheromones, indicating the shortest path between food and the nest (Dorigo and Blum, 2005). The stronger pheromones in a path, the more ants have selected that path for moving. The process of selecting a path by an ant is probabilistic. The algorithm uses a probability density function with a Gaussian kernel. When a new solution is added to the archive, the worst of the solutions is removed. After reaching a certain number of iterations, the best path is considered the best optimization result.

The differential evolution (DE) is based on a differential operator to generate new solutions exchanging information among the members of the population. All members of a population have an equal chance of being selected as a parent. The generation of the children is compared to the parent's generation considering the objective function. The best members enter the next generation, while the rest are removed. DE is based on adjusting the mutation, crossover, and selection to reach the optimal point (Price et al., 2006).

Genetic algorithm (GA) optimization works based on considering an initial set of random solutions called populations. Each individual is a chromosome, representing a solution for the problem. This method selects individuals with higher eligibility, being more likely to survive and crossover (Mirjalili, 2019). After several generations, the parent chromosomes produce better offspring by removing weak solutions based on the objective function. Decision-making variables are similar to genes, a combination of which provides an answer as a chromosome-like string during the optimization.

According to Dian et al. (2019), it seems that better results can be obtained by simultaneous optimization of all three prior terms, i.e., sparsity, spectral, and spatial prior terms. Therefore, this study aims to simultaneously optimize the regularization parameters of prior terms in a sparse coding image fusion framework to create an HR-MS from input LR-MS and Pan images.

2. The Proposed Method

The fusion problem can be written in the form of multiplication of spectral basis (D) and coefficients (A) to estimate the LR-MS (Y) and Pan (Z) (Eq. 1)

$$\begin{aligned} &Y=D\times A\times S\otimes B,\\ &Z=R\times D\times A \end{aligned} \tag{1}$$

where B is the blurring matrix that models the physical constraints of the LR MS sensor using the nominal point spread function (PSF) of the imaging sensor, and S is the spatial Downsampling matrix. R is a transformation matrix from multispectral to panchromatic. Since the Pan and LR MS still preserve spectral information and spatial information, respectively, the spectral basis and coefficients can be estimated from both LR-MS and Pan. Therefore, the fusion problem can be written as Eq. (2).

$$\min_{D,A} \left\|Y-(D\times A\times S\otimes B)\right\|_F^2+\left\|Z-(R\times D\times A)\right\|_F^2 \tag{2}$$

The optimizations for D and A are severely ill posed, and they do not have a unique solution. Therefore, some prior information of the unknown HR-MS is required to regularize it. Similar to Dian et al. (2019), three essential prior terms, i.e., sparsity prior term, nonlocal similarities, and prior terms of spectral unmixing, were incorporated into a unified framework. A flowchart of the proposed approach is presented in Figure 1.

Sparsity prior term is effective for dealing with various hyperspectral reconstruction problems (Lu et al., 2016). This prior term assumes each spectral pixel in a high spectral resolution image can be expressed as the linear combination of a few distinct spectral signatures. In this situation, each column of the coefficients A can be sparse if an appropriate spectral basis is available. The sparsity prior term can be added to Eq. (2) as Eq. (3)

$$\min_{D,A} \left\|Y-(D\times A\times S\otimes B)\right\|_F^2+\left\|Z-(R\times D\times A)\right\|_F^2+\eta_1\left\|A\right\|_1 \tag{3}$$

where $||A||_1$ stands for the sum of absolute values of all elements of A, and η_1 is the regularization parameter of sparsity prior term. A typical natural scene usually contains a collection of similar pixels from all over the image, and these nonlocal similarities can be effective for image recovery (Dong et al., 2011).

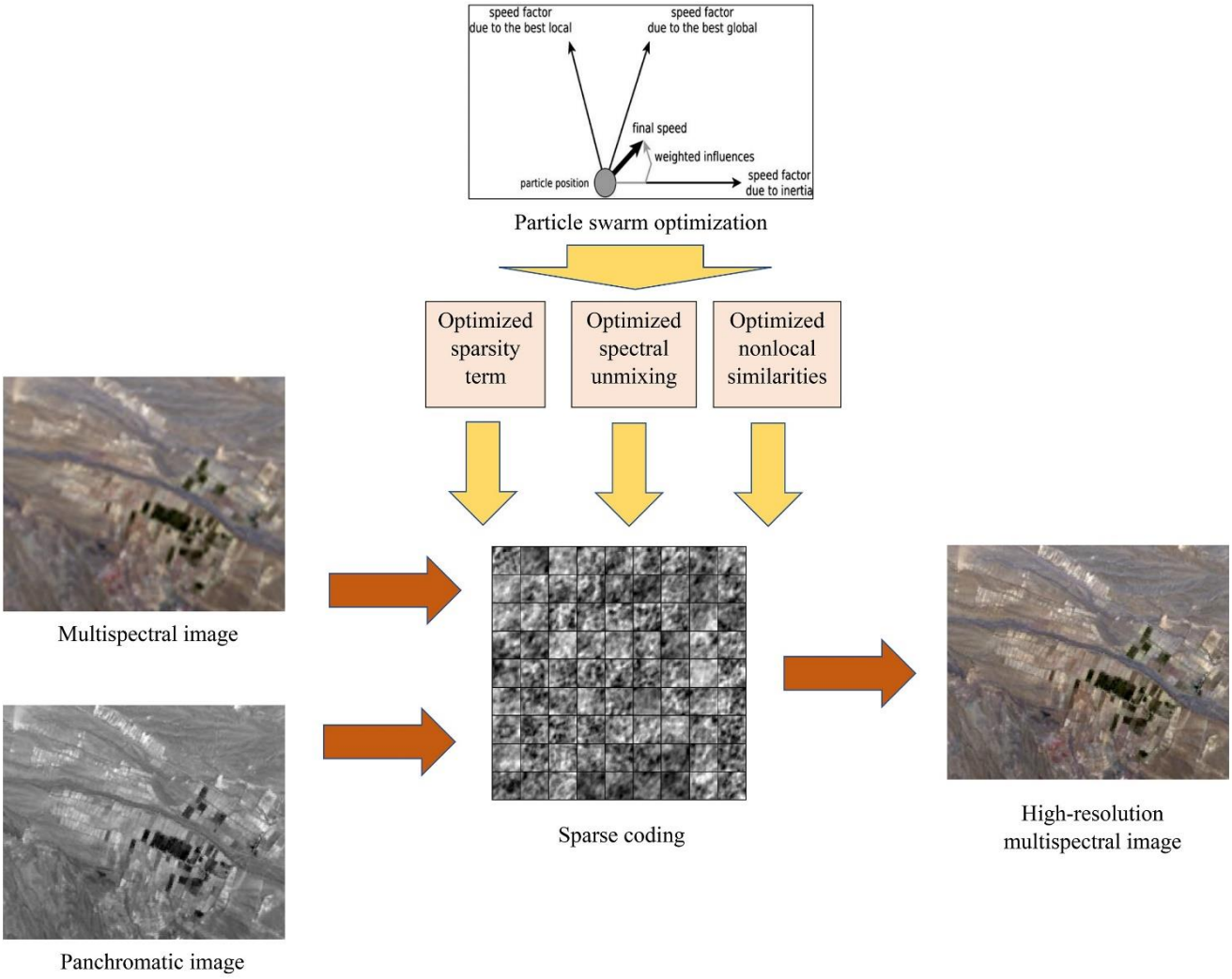

Figure 1. Flowchart of the proposed approach

To exploit the nonlocal similarities in the HR-MS, it is assumed that a pixel x_i in the HR-MS can be approximated by a linear combination of pixels, which are similar to x_i. Incorporating this prior term, a nonlocal spatial prior term can be added to the optimization problem (Eq. 4)

$$\min_{D,A}\|Y-(D\times A\times S\otimes B)\|_F^2+\|Z-(R\times D\times A)\|_F^2 \\ +\eta_1\|A\|_1+\eta_2\sum_{i=1}^{N}\|D\times A-W\times D\times A\|_F^2 \quad (4)$$

where η_2 is the regularization parameter of the spatial prior term. The vector W includes w_{ij}, which is the weighting coefficient based on the similarity between the pixel x_i and x_j. The pixels x_i and x_j are not known, and the weighting coefficients can be obtained from the Pan image since this image preserves the most spatial information of the HR-MS. To do this, the fuzzy C-Mean algorithm was performed for clustering on the Pan image to search for nearest neighbors for each pixel z_i.

The third prior term used in this study was the spectral prior term. Definition of this prior term helps to achieve better results over the regions with highly spectral variations such as heterogeneous regions, where the most spectral mixing happens. To define the prior term of spectral unmixing, the coefficient vectors satisfy the nonnegativity and sum-to-one constraints (Iordache et al., 2011). Therefore, A should be a nonnegative matrix. As the spectral basis represents the reflectance of distinct materials, each element of the spectral basis is in the range of [0,1]. Eq. (5) shows the main optimization problem considering all three types of prior information.

$$\min_{D,A}\|Y-(D\times A\times S\otimes B)\|_F^2+\|Z-(R\times D\times A)\|_F^2 \\ +\eta_1\|A\|_1+\eta_2\sum_{i=1}^{N}\|D\times A-W\times D\times A\|_F^2 \quad (5) \\ \text{s.t.}\quad 0\le D\le 1\quad\text{and}\quad 0\le A$$

In this formulation, the prior terms of sparsity, spectral unmixing, and nonlocal similarities are incorporated into a unified framework. This optimization problem is highly nonconvex, and the solution is not unique. Similar to an approach presented by Dian et al. (2019), A was updated while D was considered constant, and then D was updated while A was considered constant. These two steps were

iterated for convergence. Finally, the desired HR-MS was obtained by the multiplication of D and A.

In the optimization problem, there are three variables that their values affect the performance of the image fusion method: the size of matrix D, η_1, and η_2. Several evolutionary optimization methods were used to find the optimized values of D, η_1, and η_2. The objective function was to maximize the peak signal to noise ratio (PSNR), which is defined as the average PSNR of all bands for MS (Eq. 6),

$$\mathrm{PSNR}\left(\hat{\mathrm{X}},\mathrm{X}\right)=\frac{1}{S}\sum_{j=1}^{S}\mathrm{PSNR}\left(\hat{\mathrm{X}}^{i},\mathrm{X}^{i}\right) \quad (6)$$

where X^{i} and $\hat{\mathrm{X}}^{i}$ denote i^{th} spectral band of ground truth and estimated MS, respectively, and both of them are scaled to the range [0,255]. The PSNR measures the similarity between the ground truth image and the reconstructed image. The higher the PSNR, the better the fusion result. Other quality metrics were also used along with PSNR to assess the performance of the proposed fusion method compared to traditional and new fusion methods. These methods are relative dimensionless global error in synthesis (ERGAS) (Wald, 2002), universal image quality index (UIQI) (Wang and Bovik, 2002), spectral angle mapper (SAM) (Nencini et al., 2007). In this study, PSO, ACO, DE, and GA were used to optimize the variables to improve the performance of the fusion task. Table 1 shows the parameters and specifications of the optimization methods. A description of parameters and specifications of conventional evolutionary optimization methods is provided by Ab-Wahab et al. (2015).

Table 1. Parameters and specifications of the evolutionary optimization methods

Method	Parameter	Value
PSO	Maximum number of iterations	100
	Maximum number of particles	1000
	Initial inertia weight ($W_{\min}$)	1
	Inertia weight damping ratio (W_{damp})	0.99
	Cognitive acceleration (C_1)	1
ACO	Population size	20
	Maximum number of generations	500
	Deviation distance rate	1
	Maximum number of epochs	1000
DE	Population size	20
	Maximum number of generations	200
	Lower bound of scaling factor ($\beta_{\min}$)	0.2
	Upper bound of scaling factor ($\beta_{\max}$)	0.8
	Crossover probability (P_{CR})	0.1
	Maximum number of epochs	300
GA	Population size	100
	Maximum number of generations	500
	Mutation rate	0.1
	Crossover percentage	0.5
	Maximum number of epochs	500

3. Dataset Description

The regularization parameters of the implemented image fusion method were optimized for the fusion of actual satellite images acquired over Alberta (55° 0’ N, 115° 0’ W) during summer 2020 (Figure 2).

These satellite images have been selected with a remarkable variety of land-use/land-cover for fusion purposes. Level-2 Pan and MS bands of the Landsat-8 OLI images were used for the fusion. Level-2 OLI images consist of surface reflectance data with nine spectral bands. They have a spatial resolution of 15 m for Pan (8th spectral band) and 30 m for MS (spectral bands 1 to 9 except for 8). All spectral bands are geo-referenced using orbit and altitude data from the satellite.

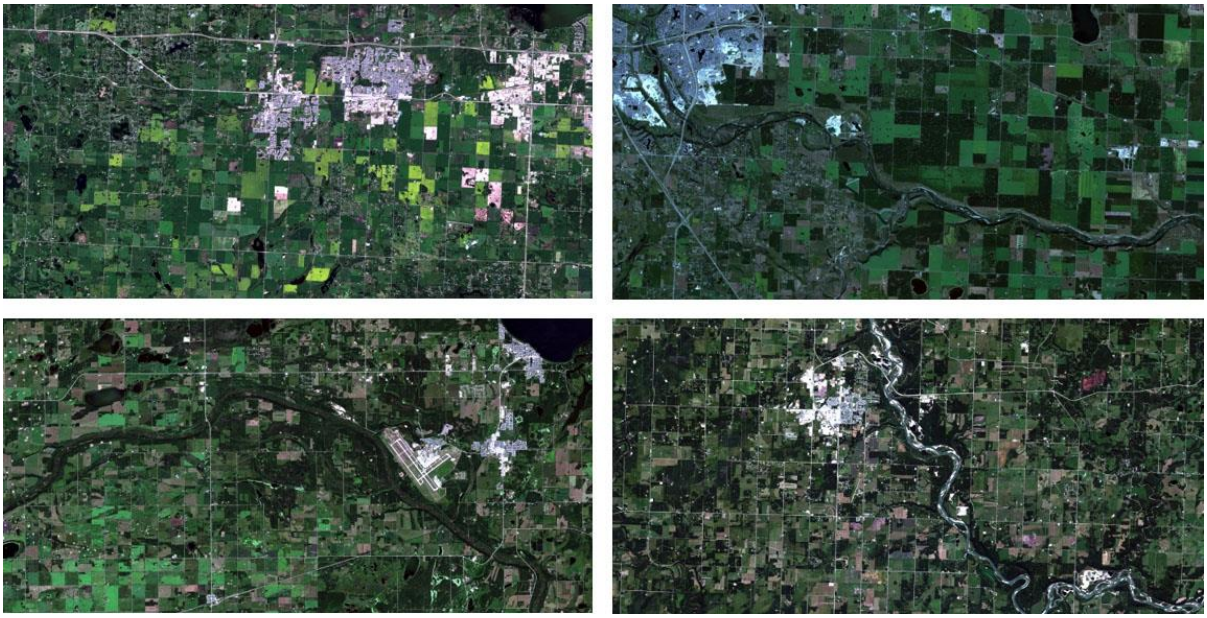

Figure 2. Satellite images of Alberta acquired during summer 2020.

4. Experimental Results

In this study, four optimization methods, namely, PSO, ACO, DE, and GA, have been used to provide the most efficient values of regularization parameters for the prior information in a sparse coding-based image fusion technique. The three regularization parameters should be optimized to achieve the most reliable fusion results. The former studies have presented the suitable value of each parameter by considering the other two parameters as constant (Dian et al., 2019). Table 2 shows the optimized values of the regularization parameters obtained by the implemented optimization methods. As can be seen in Table 2, various optimization methods have resulted in different values for the size of matrix D, η_1, and η_2. This caused various PSNR values obtained by the sparse coding image fusion based on sparsity, spatial, and spectral prior terms to creating the HR-MS image.

Table 2. Optimized values of the regularization parameters obtained by the studied optimization methods

	Method	Size of D	η_1	η_2	PSNR
Image 1	PSO	65	0.0004	0.002	62.43
	ACO	64	0.0003	0.007	58.43
	DE	65	0.0005	0.003	60.55
	GA	61	0.00008	0.002	61.53
Image 2	**PSO**	**63**	**0.0005**	**0.006**	**63.01**
	ACO	63	0.0003	0.009	58.84
	DE	68	0.0005	0.005	59.21
	GA	63	0.0001	0.001	59.77
Image 3	PSO	61	0.0005	0.004	59.78
	ACO	63	0.0003	0.007	57.71
	DE	70	0.0007	0.004	55.84
	GA	60	0.0001	0.003	57.29
Image 4	PSO	63	0.0004	0.005	60.06
	ACO	62	0.0002	0.008	58.33
	DE	69	0.0006	0.008	58.00
	GA	63	0.0002	0.003	58.53

According to Table 2, PSO has resulted in the highest PSNR values on the study dataset. The algorithm was implemented to fuse LR-MS and Pan images to create four HR-MS images. For the studied optimization algorithms, the optimized size of matrix D varied between 61 and 70, optimized η_1 varied between 0.00008 and 0.0007, and optimized η_2 varied between 0.001 and 0.009. The highest PSNR value was 63.01, obtained from the size of matrix D

of 63, η_1 of 0.0005, and η_2 of 0.006. The PSNR value approaches infinity as the mean square error (MSE) approaches zero; this shows that a higher PSNR value implies a higher image quality. At the other end of the scale, a small value of the PSNR implies high numerical differences between images.

Several methods, including the sparse approach proposed by Dian et al. (2019), Gram-Schmidt (GS) (Laben and Brower, 2000), Brovey transform (BT) (Jiang et al., 2011), generalized intensity-hue-saturation (GIHS) (Tu et al., 2001), and smoothing filter-based intensity modulation (SFIM) (Liu, 2000) were implemented, and their results on the dataset were investigated (Figure 3).

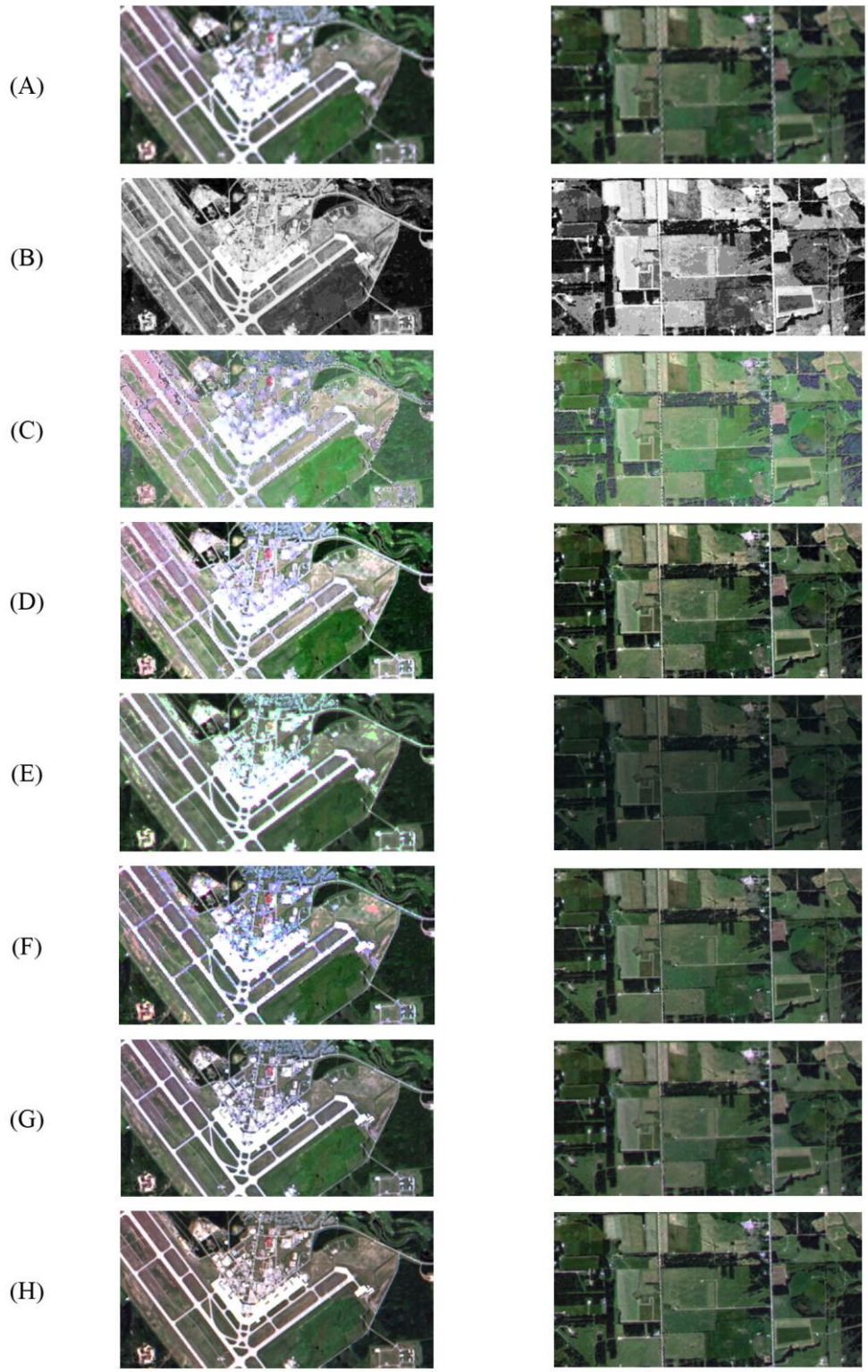

Figure 3. (A) input MS, (B) input PAN, (C to H) Fused images using GIHS, SFIM, GS, BT, Sparse, and the proposed OSC method, respectively

The results of ERGAS, SAM, UIQI, and PSNR values obtained by different methods are presented in Figure 4 to Figure 7. OSC stands for optimized sparse coding, which is introduced in this study. The average PSNR values on the images of the study area using the OSC approach was 62.12, which was higher than that of the other methods. The implemented methods are among the efficient image fusion algorithms. Implemented classic fusion methods resulted in PSNR values lower than that of OSC. According to Figure 4 toFigure 7, the proposed fusion method showed better values for ERGAS, SAM, UIQI, and PSNR than the sparse approach proposed by Dian et al. (2019), which is due to the proposed strategy for the optimization problem. This means that the proposed OSC approach can preserve spatial details while eliminating spectral distortions. The reason for efficient image fusion results using the OSC approach is that the spectral basis and sparse coefficients are estimated from the LR-MS and Pan by exploiting the nonlocal self-similarities, prior knowledge of the spectral unmixing, and a sparsity prior term. A typical natural scenario is often self-similar, and therefore it usually contains similar pixels from all over the image, which has been proved to be effective for image restoration. Besides, based on the spectral mixture model, the spectral basis and coefficients are nonnegative, and the coefficients often satisfy the sum-to-one constraint. Furthermore, under the appropriate spectral basis, the coefficients can be sparse, which is helpful in many multispectral image reconstruction problems.

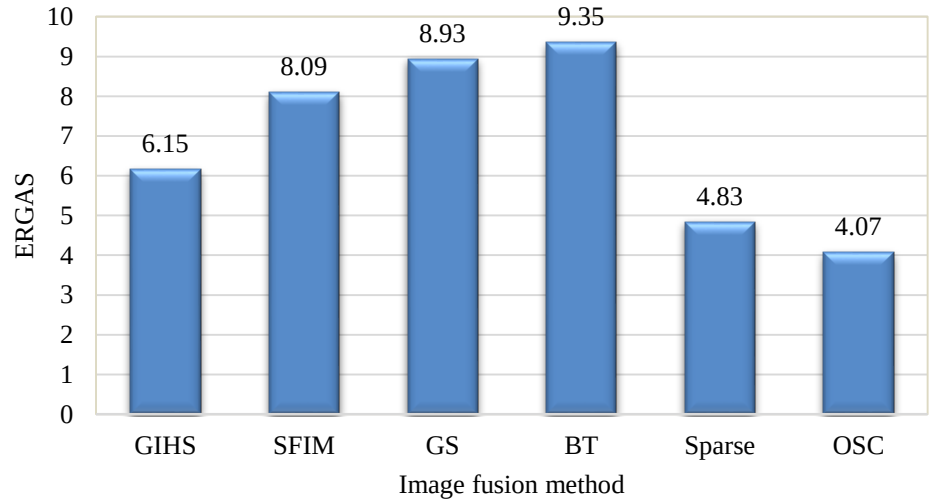

Figure 4. Average ERGAS values obtained from different fusion methods over input images

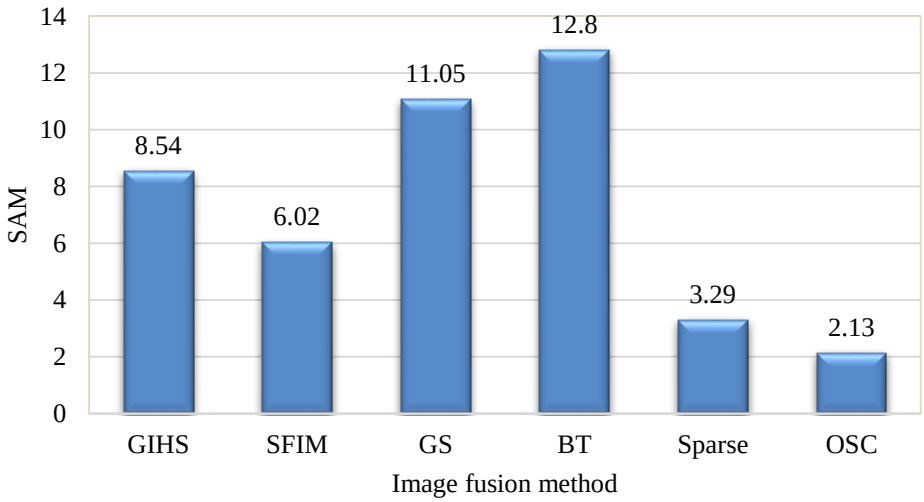

Figure 5. Average SAM values obtained from different fusion methods over input images

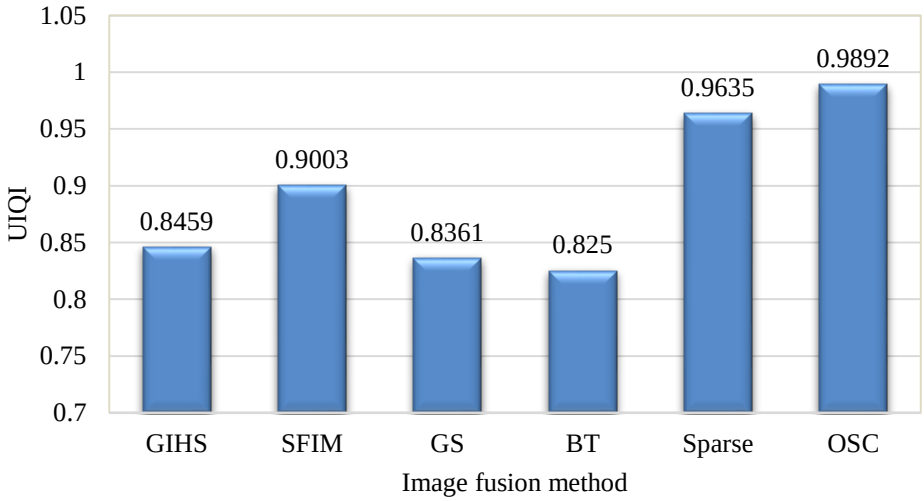

Figure 6. Average UIQI values obtained from different fusion methods over input images

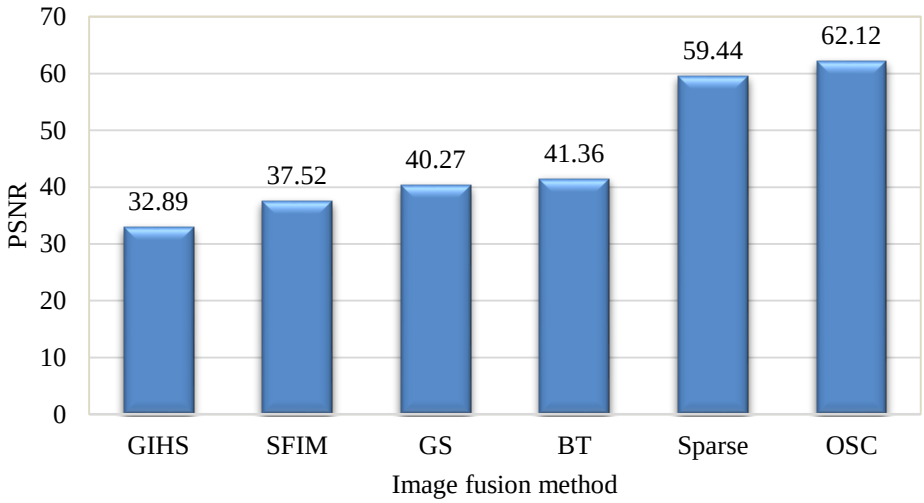

Figure 7. Average PSNR values obtained from different fusion methods over input images

5. Conclusions

Several optimization algorithms were introduced to optimize the regularization parameters of sparsity, spatial, and spectral prior terms in sparse coding-based multispectral image fusion prior terms, among which, PSO resulted in the highest PSNR values (63.01) on the studied dataset. The findings of this study show that better fusion results could be obtained by simultaneous optimization of the prior terms. The main benefit of the proposed OSC approach compared to conventional fusion methods is the outstanding ability to preserve spatial details while eliminating spectral distortions. This is due to considering nonlocal similarities from all over the image instead of focusing on the neighboring pixels. The object-based approach toward the fusion problem in the proposed method is the key to achieve more reliable results over more heterogeneous regions and eliminate spectral distortions. The results of this study can be used in sparse coding-based image fusion methods to create HR-MS images.

References

Ab-Wahab, M. N., Nefti-Meziani, S. & Atyabi, A. (2015). "A comprehensive review of swarm optimization algorithms." PLoS ONE **10**(5): 1–36.

Akhtar, N., Shafait, F. & Mian, A. (2014). Sparse spatio-spectral representation for hyperspectral image super-resolution. In European conference on computer vision, 63 78. Springer, Cham.

Akhtar, N., Shafait, F. & Mian, A. (2015). Bayesian sparse representation for hyperspectral image super resolution. In Proceedings of the IEEE conference on computer vision and pattern recognition, 3631–3640.

Dadrass Javan, F., Samadzadegan, F., Mehravar, S., Toosi, A., Khatami, R. & Stein, A. (2021). "A review of image fusion techniques for pan-sharpening of high-resolution

satellite imagery." ISPRS Journal of Photogrammetry and Remote Sensing **171**: 101–117.

Dian, R., Li, S., Fang, L. & Wei, Q. (2019). "Multispectral and hyperspectral image fusion with spatial-spectral sparse representation." Information Fusion **49**: 262–270.

Dong, W., Fu, F., Shi, G., Cao, X., Wu, J., Li, G. & Li, X. (2016). "Hyperspectral image super-resolution via nonnegative structured sparse representation." IEEE Transactions on Image Processing **25**(5): 2337–2352.

Dong, W., Li, X., Zhang, L. & Shi, G. (2011). Sparsity-based image denoising via dictionary learning and structural clustering. In CVPR 2011, 457–464. IEEE.

Dorigo, M. & Blum, C. (2005). "Ant colony optimization theory: A survey." Theoretical computer science **344**(2–3): 243–278.

Eghbalian, S. & Ghassemian, H. (2018). "Multispectral image fusion by deep convolutional neural network and new spectral loss function." International Journal of Remote Sensing **39**(12): 3983–4002.

Gunatilaka, A. H. & Baertlein, B. A. (2001). "Feature-level and decision-level fusion of noncoincidently sampled sensors for land mine detection." IEEE transactions on pattern analysis and machine intelligence **23**(6): 577–589.

Hardie, R. C., Eismann, M. T. & Wilson, G. L. (2004). "MAP estimation for hyperspectral image resolution enhancement using an auxiliary sensor." IEEE Transactions on Image Processing, **13**(9): 1174–1184.

Iordache, M. D., Bioucas-Dias, J. M. & Plaza, A. (2011). "Sparse unmixing of hyperspectral data." IEEE Transactions on Geoscience and Remote Sensing **49**(6): 2014–2039.

Jiang, D., Zhuang, D., Huang, Y. & Fu, J. (2011). "Survey of multispectral image fusion techniques in remote sensing applications." Image Fusion and Its Applications, 1–23.

Kawakami, R., Matsushita, Y., Wright, J., Ben-Ezra, M., Tai, Y. W. & Ikeuchi, K. (2011). High-resolution hyperspectral imaging via matrix factorization. In CVPR 2011, 2329–2336. IEEE.

Kaur, G., Saini, K. S. & Singh, D. (2021). "A comprehensive study on computational pansharpening techniques for remote sensing images." Archives of Computational Methods in Engineering **28**(2): 1–18.

Kulkarni, S. C. & Rege, P. P. (2020). "Pixel level fusion techniques for SAR and optical images: A review." Information Fusion **59**: 13–29.

Laben, C. A. & Brower. B. V. (2000). "Process for enhancing the spatial resolution of multispectral imagery using pan-sharpening." US Patent 6,011,875.

Li, J., Qiu, T., Wen, C., Xie, K. & Wen, F. Q. (2018). "Robust face recognition using the deep C2D-CNN model based on decision-level fusion." Sensors **18**(7): 2080.

Li, S., Kang, X., Fang, L., Hu, J. & Yin, H. (2017). "Pixel-level image fusion: A survey of the state of the art." information Fusion **33**: 100–112.

Liu, J. G. (2000). "Smoothing filter-based intensity modulation: a spectral preserve image fusion technique for improving spatial details." International Journal of Remote Sensing **21**(18): 3461–3472.

Lu, T., Li, S., Fang, L., Ma, Y. & Benediktsson, J. A. (2016). "Spectral–spatial adaptive sparse representation for hyperspectral image denoising." IEEE Transactions on Geoscience and Remote Sensing **54**(1): 373–385.

Metwalli, M. R., Nasr, A. H., Allah, O. S. F. & El-Rabaie, S. (2009). Image fusion based on principal component analysis and high-pass filter. In 2009 International Conference on Computer Engineering & Systems, 63–70.

Mirjalili, S. (2019). "Genetic algorithm." In Evolutionary algorithms and neural networks, 43–55. Springer, Cham.

Nencini, F., Garzelli, A., Baronti, S. & Alparone, L. (2007). "Remote sensing image fusion using the curvelet transform." Information Fusion **8**(2): 143–156.

Nirmala, D. E. & Vaidehi, V. (2015). Comparison of Pixel-level and feature-level image fusion methods. In 2015 2nd international conference on computing for sustainable global development (INDIACom), 743–748. IEEE.

Price, K., Storn, R. M. & Lampinen, J. A. (2006). "Differential evolution: a practical approach to global optimization." Springer Science & Business Media.

Rajah, P., Odindi, J. & Mutanga, O. (2018). "Feature-level image fusion of optical imagery and Synthetic Aperture Radar (SAR) for invasive alien plant species detection and mapping." Remote Sensing Applications: Society and Environment **10**: 198–208.

Song, H., Huang, B., Zhang, K. & Zhang, H. (2014). "Spatio-spectral fusion of satellite images based on dictionary-pair learning." Information Fusion **18**: 148–160.

Tu, T. M., Su, S. C., Shyu, H. C. & Huang, P. S. (2001). "A new look at IHS-like image fusion methods." Information Fusion **2**(3): 177–186.

Wald, L. (2002). "Data fusion: Definitions and architectures: Fusion of images of different spatial resolutions." Les Presses de l'Ecole des Mines, Paris, France.

Wang, Z. & Bovik, A. C. (2002). "A universal image quality index." IEEE Signal Processing Letters **9**(3): 81–84.

Wei, Q., Dobigeon, N. & Tourneret, J. Y. (2015). "Fast fusion of multi-band images based on solving a

Sylvester equation." IEEE Transactions on Image Processing **24**(11): 4109–4121.

Witharana, C., Bhuiyan, M. A. E., Liljedahl, A. K., Kanevskiy, M., Epstein, H. E., Jones, B. M., Daanen, R., Griffin, C. G., Kent, K. & Jones, M. K. W. (2020). "Understanding the synergies of deep learning and data fusion of multispectral and panchromatic high-resolution commercial satellite imagery for automated ice-wedge polygon detection." ISPRS Journal of Photogrammetry and Remote Sensing **170**: 174–191.

Xiao, G., Bavirisetti, D. P., Liu, G. & Zhang, X. (2020a). Decision-Level Image Fusion. In Image Fusion, 149–170. Springer, Singapore.

Xiao, G., Bavirisetti, D. P., Liu, G. & Zhang, X. (2020b). Feature-Level Image Fusion. In Image Fusion, 103–147. Springer, Singapore.

Xu, Y., Wu, Z., Chanussot, J. & Wei, Z. (2019). "Nonlocal patch tensor sparse representation for hyperspectral image super-resolution." IEEE Transactions on Image Processing **28**(6): 3034–3047.

Yang, X. S. (2020). "Nature-inspired optimization algorithms: Challenges and open problems." Journal of Computational Science **46**: 1–8.

Yilmaz, C. S., Yilmaz, V. & Güngör, O. (2020). "On the use of the SOS metaheuristic algorithm in hybrid image fusion methods to achieve optimum spectral fidelity." International Journal of Remote Sensing **41**(10): 3993–4021.

Zhang, Y. (2004). "Understanding image fusion." Photogrammetric Engineering & Remote Sensing **70**(6): 657–661.